Gait & Posture 113 (2024) 40–45

Contents lists available at ScienceDirect

Gait & Posture

journal homepage: www.elsevier.com/locate/gaitpost

Multivariate functional principal component analysis and k-means clustering to identify kinematic foot types during gait in children with cerebral palsy

Eric L. Dugan [a,b,*], Amy E. Barbuto [a], Cara M. Masterson [a], Jeffrey Shilt [a,b]

[a] Texas Children's Hospital, The Woodlands, TX 77384, USA
[b] Department of Orthopedic Surgery, Baylor College of Medicine, Houston, TX 77030, USA

ARTICLE INFO

Keywords:
Classification
3D gait analysis
Equinopronovalgus
Equinosupovarus

ABSTRACT

Background: Children with neuromuscular disorders, such as cerebral palsy, frequently develop foot deformities, such as equinopronovalgus and equinosupovarus, leading to walking difficulties and discomfort. Traditional assessment methods, including clinical measures and radiographs, often fail to capture the dynamic nature of these deformities, resulting in suboptimal treatment. 3D gait analysis using multisegment foot models offers a more detailed understanding of these deformities.
Research question: To determine whether the combination of multisegment foot models, multivariate functional principal component analysis, and k-means cluster analyses could identify distinct, clinically relevant foot types in a large pediatric cohort with cerebral palsy.
Methods: This was a retrospective analysis of 3D gait data from 197 patients with cerebral palsy collected using a multisegment foot model. Multivariate functional principal component analysis was used to reduce these data prior to using k-means clustering to identify foot posture clusters. Further analyses, including ANOVA and Fisher's Exact tests, were used to evaluate demographic, radiographic, and gait characteristics to explain the clinical relevance of each cluster.
Results: Analysis of kinematic data from 371 feet revealed six clinically significant clusters, with a low misclassification rate of 2 %. One-factor ANOVAs demonstrated significant differences across clusters for all MPCs, whereas no significant differences were noted in basic anthropometric variables. Significant variations were observed in radiographic and gait function variables, and a strong association between GMFCS levels and cluster categorization was identified.
Significance: The novel approach of integrating multivariate functional principal component analysis and k-means clustering identified a spectrum of foot deformities in children with CP, ranging from equinosupovarus to marked equinopronovalgus. This methodology provides an objective classification based on kinematic data and can facilitate improved diagnosis and treatment of cerebral palsy-related foot deformities.

1. Introduction

Children with neuromuscular disorders frequently develop foot deformities due to underlying impairments, leading to impaired walking pattern, skin irritation, pain, and difficulty wearing shoes or orthotics. These deformities can be categorized into three levels: dynamic soft tissue imbalances, fixed soft tissue imbalances, and fixed soft tissue imbalances with skeletal malalignment [1]. Imbalances manifest as varied intersegmental positioning of the foot, ranging from equinopronovalgus to equinosupovarus, and are characterized by distinct hindfoot, midfoot, and forefoot orientations [1,2]. Classifying foot types within this spectrum poses challenges, especially for those not at the extremes.

For example, Hamel and colleagues could not distinguish between children with flat and normal feet using static radiographic measures alone [5]. When comparing static radiographs to dynamic foot function, Bohm et al. found that in children with common types of foot deformities, static radiographic alignment only accounts for a small amount of the variance in foot kinematics [6]. Similarly, clinical examinations of foot posture are not always consistent with kinematic

* Correspondence to: Texas Children's Hospital, 17580 Interstate 45 South, The Woodlands, TX 77384, USA.
E-mail address: eldugan@texaschildrens.org (E.L. Dugan).

https://doi.org/10.1016/j.gaitpost.2024.05.032
Received 3 December 2023; Received in revised form 3 April 2024; Accepted 28 May 2024
Available online 1 June 2024

assessements of dynamic foot motion [7,8]. Kruger and colleagues [3] found that children with planovalgus feet showed significant variability in hindfoot alignment in the coronal plane, from marked eversion to inversion, while Amene et al. identified four distinct variations of planovalgus feet using a multisegment foot model [4]. The limitations of relying solely on radiographic measures and the diversity of foot alignments within clinical categories complicate the development of effective treatment strategies and suggest that there are a spectrum of deviations from typical foot alignment rather than distinct categories of deformities.

To overcome these challenges, multisegment foot models integrated into 3D gait analysis have emerged as a promising solution. These models offer detailed insight into the dynamic interactions of different foot segments during walking, facilitating more effective treatment decision-making and tailored interventions. Previous studies have successfully used multisegment foot models in conjunction with principal component analysis (PCA) and k-means cluster analysis to classify foot deformities such as equinovarus and planovalgus [4,9,10].

While using multisegment foot models and clustering algorithms has shown promise in classifying foot deformities, there are still gaps in the literature regarding the use of these techniques. The goal of the the current study was to extend the prior work of Krzak, Amene, and Bohm [4,9,10] by analyzing a larger, more diverse group of patients using multivariate PCA paired with k-means clustering analysis to determine whether these methods could successfully identify distinct and clinically relevant foot types in children with cerebral palsy (CP). This approach has the potential to improve the identification of functional foot deformities and inform strategies for managing and treating these foot deformities.

2. Methods

This retrospective analysis was based on a convenience sample of 197 pediatric patients who had a primary diagnosis of CP and underwent instrumented 3D gait analysis in our laboratory. Specifically, this included all patients twenty-one years of age or younger and all types of cerebral palsy regardless of topographical distribution or tone type. All patients included in the study completed a barefoot gait analysis following a standardized protocol that included the use of the multi-segment Istituto Orthopedico Rizzoli (IOR) foot model[11]. To assist with the interpretation of the subsequent cluster analyses, only feet for which standard radiographs were obtained during clinical visits were included in the analysis. The investigators' institutional review board approved this protocol, and because all data were collected as standard medical care, a waiver of informed consent was granted.

2.1. Data collection and processing

A Vicon Nexus system (Vicon Motion Systems Ltd., Oxford, UK) with 12 Vantage cameras was used to capture foot kinematics during barefoot walking at a self-selected speed along a 10-m walkway. Markers were placed according to the modified IOR foot model to measure foot and ankle motion [11]. This model includes five segments: shank, calcaneus, midfoot, metatarsus, and hallux. Marker data were sampled at 120 Hz, and force plate data were sampled at 1000 Hz via six force plates (AMTI Inc., Watertown MA, USA). All data processing was performed in Visual 3D (C-Motion, Inc., Germantown, MD). Marker trajectories and ground reaction force data were filtered using a low-pass Butterworth filter with cut-off frequencies of 6 and 25 Hz, respectively.

The foot segment angles included in the analysis were dorsiflexion, eversion, and adduction of both the Sha-Cal (shank to calcaneus) and Cal-Met (calcaneus to metatarsus) joints. The examination of these joint angles is supported by prior literature that documented significant joint angle alterations detected using multisegment foot model kinematics in planovalgus feet [12–14]. These angles align with the observed location of deformity in planovalgus feet on weight bearing radiographs [15] and are consistent with clinical definitions of planovalgus and cavovarus foot deformity [16].

2.2. Multivariate functional principal component analysis

Multivariate functional principal component analysis (MFPCA) formed the basis of our analysis, enhancing traditional functional principal component analysis (fPCA) for multivariate functional data. This data, evolving over continuous domains such as time, comprises multiple correlated functions. MFPCA identifies dominant patterns in these datasets by decomposing their covariance function into principal components, known as multivariate principal components (MPCs). These MPCs capture primary variations in the data and reduce its dimensionality, accounting for correlations across variables or functions. This reduction facilitates visualization and interpretation of MPCs, simplifying further analysis such as clustering or regression.

The application of MFPCA in gait data analysis [17,18] addresses the limitations of univariate fPCA. fPCA indirectly captures covariation across multiple joints, which often makes interpretation of results difficult due to high principal component score correlations and potential multicollinearity issues [19]. In contrast, MFPCA directly addresses joint covariation, thereby revealing the essential characteristics of complex joint movement patterns. MFPCA aligns naturally with the structure of multivariate functional data, enabling a more meaningful representation of observations.

Joint angle data were organized into a MultiFunData object in R, with each component representing one joint angle. These angles, averaged over six strides and normalized to the stance phase of the gait cycle, formed the rows of each component, with columns representing 0 %–100 % of stance. MFPCA was performed in R [20] using the fda and MPFCA R packages [19,21–23]. The first four principal components, accounting for over 90 % of the variance, were used as inputs for the k-means clustering analysis. A bootstrap with replacement analysis was used to assess the stability and reliability of the eigenvalues derived from the MFPCA. The results of this analysis and the graphical representation of the variance accounted for by each principal component are presented in Appendix A.

2.3. Clustering analysis

To establish an appropriate number of clusters for our k-means analysis, we used the elbow method with a limit of 20 potential clusters. For each cluster number ranging from 1 to 20, k-means clustering was performed, and the total within-cluster sum of squares (WSS) was calculated. Plotting these WSS values against the number of clusters allowed us to identify the 'elbow point,' which occurs when the addition of more clusters does not lead to a significant reduction in WSS. This analysis revealed that the variance in the data markedly decreased after six clusters, leading us to select this number for our subsequent K-means clustering.

To validate the stability and reliability of our cluster assignments, we used a ten-fold cross-validation approach similar to that described by Rozumalski and Schwartz [24]. Initially, k-means analysis was conducted on the entire dataset to establish a reference cluster membership for each individual. The dataset was then divided into ten equal parts, with k-means analysis iteratively performed nine times on nine parts, assigning test memberships to trials in the excluded part. This process was repeated, with a different part excluded each time. The misclassification rate was calculated by comparing the reference and test memberships, providing a measure of the accuracy of our cluster configurations.

2.4. Additional analyses

Our study primarily aimed to explore whether multisegment foot kinematics in patients with CP could categorize distinct, clinically relevant foot types. Following the clustering analysis, we conducted secondary analyses on demographic, radiographic, and gait data to better understand the clinical attributes of each cluster.

We used one-factor ANOVAs to examine differences in variables such as age, height, mass, and several specific foot and gait metrics, including calcaneal pitch (CalPitch), naviculocuboid overlap (NCO), talonavicular coverage angle (TNC), anteroposterior talo-first metatarsal angle (APTaloFirstMet), tibiotalar angle (TibioTalar) [25], gait deviation index (GDI), and peak ankle power normalized to body mass, setting the alpha level at 0.05. Significant differences found via ANOVAs led to further post hoc comparisons using Tukey's HSD test, with a significance threshold of $p < 0.05$. Similar to Bohm et al. [9], we treated each foot independently in our analyses.

To assess the relationship between cluster classifications and categorical variables such as sex and GMFCS level, we applied Fisher's Exact tests, which are known for their efficacy in small sample and categorical data analysis, adhering to an $\alpha = 0.05$ significance level.

In addition, we used one-factor ANOVAs to evaluate the differences in the MPCs across clusters, enhancing our understanding of each cluster's unique features. All statistical procedures were performed using R [20].

3. Results

Kinematic data from 371 feet from 197 patients (82 female/115 male, age = 12 ± 4 yrs, height = 141 ± 20 cm, mass = 40.7 ± 19.2 kg) were included in the analysis. The analysis revealed six clinically meaningful clusters. The clustering analysis was highly repeatable, with a misclassification rate of only 2 %. This indicates that the clusters were consistently reproducible and thus effectively represent a spectrum of foot deformities and functional characteristics. The mean kinematic curves for each cluster are presented in Fig. 1, and the topographical distribution by cluster is presented in Table 1.

One-factor ANOVA revealed significant differences across clusters for each of the four MPCs. ANOVA results showed $F(5, 365) = 367.1$, $p < 0.001$ for MPC1, $F(5, 365) = 78.81$, $p < 0.001$ for MPC2, $F(5, 365) = 49.83$, $p < 0.001$ for MPC3, and $F(5, 365) = 9.317$, $p < 0.001$ for MPC4. Post hoc analyses indicated significant pairwise differences between clusters. The mean values, standard deviations, and post hoc comparison details are presented in Table 2.

Separate ANOVAs were conducted to examine differences in basic anthropometric variables of age, height, and mass across the six clusters. No significant differences across clusters for anthropometric variables were found (Age: $F(1, 195) = 0.221$, $p = 0.639$; Height: $F(1, 195) = 0.491$, $p = 0.484$; Mass: $F(1, 195) = 0.027$, $p = 0.869$). In addition, Fisher's Exact Test showed no significant association ($p = 0.5625$, two-tailed) between sex and cluster categorization. The mean values, standard deviations, and relevant post hoc comparisons for these variables are presented in Table 3.

In contrast to the demographic data, ANOVAs revealed significant differences in radiographic measures across the six clusters. Including NCO, CalPitch, TNC, APTaloFirstMet, and TibioTalar (NCO: $F(5, 357) = 74.26$, $p < 0.001$; CalPitch: $F(5, 358) = 24.33$, $p < 0.001$; TNC: $F(5, 354) = 51.25$, $p < 0.001$; APTaloFirstMet: $F(5, 350) = 48.2$, $p < 0.001$; TibioTalar: $F(5, 318) = 3.861$, $p = 0.002$). Mean values, standard deviations, and relevant post-hoc comparisons for these variables are presented in Table 3.

With respect to gait function, ANOVAs revealed significant differences in GDI and peak ankle power across the six clusters (GDI: $F(5, 365) = 7.777$, $p < 0.001$; Peak ankle power: $F(5, 271) = 7.193$, $p < 0.001$). In a related analysis, a Fisher's Exact Test showed a statistically significant association ($p < 0.001$) between GMFCS levels and cluster categorization. The mean values, standard deviations, and relevant post hoc comparisons for these variables are presented in Table 3.

4. Discussion

Using combined MFPCA and k-means clustering analyses, a spectrum

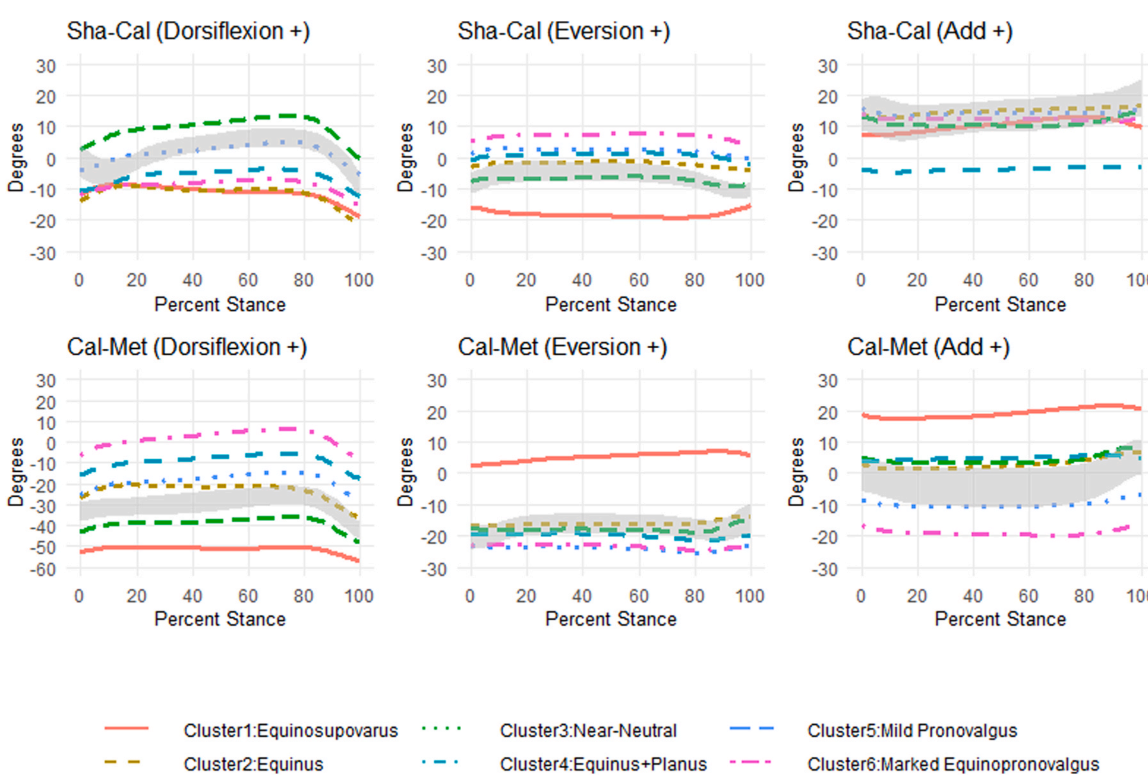

Fig. 1. Mean values for each of the six multisegment foot angles by cluster. Clusters are indicated by combination of line color and style. Gray bands represent the mean and one standard deviation of our laboratory's control data collected on typically developing children.

Table 1
Distribution of topographical classification across the six clusters.

Topographical Classification	Cluster 1	Cluster 2	Cluster 3	Cluster 4	Cluster 5	Cluster 6
Hemiplegia	15	8	10	6	17	1
Diplegia	5	11	9	22	36	15
Triplegia	1	7	5	3	6	3
Quadriplegia	1	4	2	4	4	2

Table 2
Means and standard deviations for the multivariate principal component scores are provided for each of the six clusters. In cases where ANOVAs indicated significant differences between clusters, the signficant post-hoc test results are presented, with each cluster denoted as 'C'.

Variable	Cluster 1	Cluster 2	Cluster 3	Cluster 4	Cluster 5	Cluster 6	Post-hoc combinations with significant differences
Multivariate Principal Component 1	-466 (150)	-54 (76)	-190 (99)	59 (82)	84 (65)	292 (96)	C2-C1, C3-C1, C4-C1, C5-C1, C6-C1, C3-C2, C4-C2, C5-C2, C6-C2, C4-C3, C5-C3, C6-C3, C6-C4, C6-C5
Multivariate Principal Component 2	-93 (127)	-66 (74)	142 (123)	-120 (85)	88 (80)	-41 (87)	C3-C1, C5-C1, C3-C2, C4-C2, C5-C2, C4-C3, C5-C3, C6-C3, C5-C4, C6-C4, C6-C5
Multivariate Principal Component 3	65 (149)	57 (87)	-45 (79)	-144 (99)	18 (62)	52 (64)	C3-C1, C4-C1, C3-C2, C4-C2, C5-C2, C4-C3, C5-C3, C6-C3, C5-C4, C6-C4
Multivariate Principal Component 4	43 (150)	-48 (60)	-2 (76)	23 (82)	-8 (63)	25 (57)	C2-C1, C5-C1, C3-C2, C4-C2, C5-C2, C6-C2

Table 3
Summary statistics, including means, standard deviations, and counts for patient demographics, radiographic measures, and gait variables are provided for each of the six clusters. Where ANOVAs indicated significant differences between clusters, the pair-wise post-hoc results are detailed, with clusters abbreviated as 'C'.

Parameter	Cluster 1	Cluster 2	Cluster 3	Cluster 4	Cluster 5	Cluster 6	Post-hoc combinations with significant differences
Patient Demographics							
Age (yrs)	13 (4)	9 (3)	15 (5)	10 (3)	13 (4)	11 (4)	NA
Height (cm)	145 (18)	130 (15)	151 (15)	131 (17)	147 (20)	136 (21)	NA
Mass (kg)	45 (18)	31 (14)	53 (22)	32 (14)	46 (20)	35 (15)	NA
Sex (F/M)	11/11	13/17	10/16	18/17	24/39	6/15	NA
GMFCS (I/II/III)	8/11/3	4/15/11	11/12/3	5/21/9	14/37/12	1/6/14	NA
Radiographic Measures							
Calcaneal Pitch (deg)	17 (9)	9 (5)	17 (7)	7 (5)	11 (7)	6 (5)	C2-C1, C4-C1, C5-C1, C6-C1, C3-C2, C4-C3, C5-C3, C6-C3, C5-C4, C6-C5
Naviculocuboid Overlap (%)	11 (19)	62 (17)	42 (28)	69 (18)	70 (20)	86 (17)	C2-C1, C3-C1, C4-C1, C5-C1, C6-C1, C3-C2, C6-C2, C4-C3, C5-C3, C6-C3, C6-C4, C6-C5
Talonavicular Coverage Angle (deg)	-12 (28)	27 (14)	8 (18)	30 (13)	27 (12)	36 (14)	C2-C1, C3-C1, C4-C1, C5-C1, C6-C1, C3-C2, C6-C2, C4-C3, C5-C3, C6-C3, C6-C5
Anteroposterior Talo-First Metatarsal Angle (deg)	-18 (35)	11 (8)	0 (16)	17 (11)	18 (9)	26 (11)	C2-C1, C3-C1, C4-C1, C5-C1, C6-C1, C3-C2, C5-C2, C6-C2, C4-C3, C5-C3, C6-C3, C6-C4, C6-C5
Tibiotalar Angle (deg)	9 (8)	4 (4)	6 (7)	5 (6)	4 (5)	3 (7)	C2-C1, C4-C1, C6-C1
Gait Variables							
Gait Deviation Index	64 (12)	69 (10)	73 (10)	71 (10)	74 (12)	65 (12)	C3-C1, C5-C1, C5-C2, C6-C3, C6-C5
Peak Ankle Power (W/kg)	1.02 (0.42)	1.61 (0.89)	1.80 (0.79)	1.27 (0.57)	1.56 (0.72)	1.00 (0.47)	C2-C1, C3-C1, C5-C1, C6-C2, C4-C3, C6-C3, C6-C5

of foot deformities in children with CP was identified and divided into six meaningful clusters. These clusters, ranging from equinosupovarus (Cluster 1) to marked equinopronovalgus (Cluster 6), each possess unique morphological and biomechanical traits that may inform clinical management. See Figures B1-B6 in Appendix B for further details on the kinematic profiles of the six foot type clusters.

This study builds on previous research by Bohm, Krzak, and Amene, who investigated kinematic foot patterns in children with specific deformities such as pes planovalgus or equinovarus [4,9,10]. However, in contrast to these studies, our research did not restrict the analysis to preselected clinically identified foot types. Rather, all foot types for patients with CP were included, and the foot type classification was based solely on multisegment foot kinematic data from standard gait analysis sessions.

4.1. Interpretation of the clinical relevance of the clusters

The first multivariate principal component (MPC1) accounts for the largest percentage of variation in the cluster analysis and differentiates the clusters based on foot type, pronovalgus versus supovarus. MPC1 essentially sets the two endpoints for the spectrum of foot types for which all six clusters fall along. MPC1 scores for all clusters are significantly different from each other except for the equinus planus and mild pronovalgus clusters. The remaining three MPCs then help delineate the subgroups or clusters along the continuum of foot deformity between these endpoints.

4.1.1. Cluster 1: equinosupovarus foot type

In cluster one, we found kinematic and radiographic results that confirmed that this cluster best represents an equinosupovarus foot type. In relation to normative radiographic values reported by Davids and colleagues [26], cluster one demonstrated near normal CalPitch and low angles for NCO, TNC, and APTaloFirstMet (Table 3). Feet in cluster one also demonstrated excessive Sha-Cal and Cal-Met plantarflexion, increased Sha-Cal inversion, Cal-Met eversion, and Cal-Met adduction in the multisegment foot kinematic data. Taken together, these characteristics align with a supinated foot position, confirming the equinosupovarus foot type.

4.1.2. Cluster 2: equinus foot type

Moving to cluster two, we found kinematic and radiographic results that confirmed this cluster as best representing an equinus foot type. This cluster demonstrated increased Sha-Cal plantarflexion and near normal alignment at all other joints and planes. This cluster demonstrated decreased CalPitch associated with an equinus deformity, with near normal values for all other radiographic measures [26], indicating the preservation of the intrinsic structural integrity of the foot. This supports the classification of this cluster as equinus because the only major departures from normal kinematic and radiographic norms are excessive Sha-Cal plantarflexion and diminished CalPitch, respectively.

4.1.3. Cluster 3: Near-neutral

The feet in cluster three demonstrated only minor deviations from normal kinematics and radiographic measures in all joints and planes of motion. In addition, this foot cluster demonstrated the highest GDI and peak ankle power values among the six clusters. Taken together, these results support that although the feet of cluster three may fall slightly outside some of the normative values expected in children without CP, they in large part present with a relatively normal morphology and function. Therefore, the data support this cluster as near neutral or minimally impaired foot type.

4.1.4. Cluster 4: equinus planus foot type

Cluster four was characterized by decreased CalPitch, moderately increased NCO, and near normal TNC and APTaloFirstMet angles. In addition, this cluster demonstrated excessive Sha-Cal plantarflexion, reduced Cal-Met plantarflexion, and Sha-Cal abduction. This cluster differs from the equinus cluster by showing a higher incidence of increased NCO and TNC angles. Despite these deviations, the equinus planus cluster kinematic and radiographic values were not as profound as those observed in clusters five and six which presented with more severe deformities. The observed deviations, although moderate, indicate a condition with significant but not severe departures from structural norms.

4.1.5. Cluster 5: mild pronovalgus foot type

The feet in cluster five demonstrated the characteristics of a pronovalgus foot. Feet in this cluster had decreased Cal-Met plantarflexion, excessive Sha-Cal eversion, and Cal-Met abduction. In addition, they had borderline diminished CalPitch, increased NCO, normal TNC, and borderline increased APTaloFirstMet angles. Overall, the mild pronovalgus cluster demonstrated a subtler degree of pronovalgus deformity than cluster six. Despite exhibiting some structural changes, these feet maintain better functional integrity than those with more severe pronovalgus conditions. This gradation highlights the varying degrees of impact that pronovalgus deformities can have on the foot's structure and function.

4.1.6. Cluster 6: marked equinopronovalgus foot type

Finally, cluster six exhibits the most pronounced equinopronovalugus deformities, including the highest NCO and TNC angles coupled with a decreased CalPitch. This is combined with the greatest degree of Sha-Cal eversion, Cal-Met dorsiflexion, and Cal-Met abduction. Overall, these findings indicate that cluster six represents a marked equinopronovalgus foot with severe tri-planar deformities, including a significantly collapsed arch and substantial deviations from typical foot biomechanics. This is further supported by low peak ankle power and GDI values, which indicate a substantial impact on function.

4.2. Clinical management implications

The implications of these findings are important for clinical practice. The framework of these clusters provides a more nuanced classification of the typical foot deformities observed in children with CP. Since the underlying goal of a majority of orthopaedic interventions in this population is to improve ambulation, the fact that these clusters were derived from gait data enhances their clinical relevance. When managing pediatric foot deformities, clinical approaches range from noninvasive conservative treatments to surgical interventions. Cluster one, which may progress to fixed soft tissue imbalances with skeletal malalignment, often requires bony and or soft tissue surgery. Cluster three, with its near neutral alignment, can serve as a control for assessing post-treatment results. Clusters two and four, which display alignment primarily related to dynamic soft tissue imbalances, could benefit from nonsurgical approaches as first line intervention. Treatment for clusters five and six is influenced by the severity of the soft tissue imbalance and magnitude of skeletal malalignment, with cluster five being a better candidate for conservative management and cluster six being more likely to necessitate surgical correction.

4.3. Limitations

The retrospective nature of this study and the single-center design may limit the generalizability of the findings. The sample size although substantial, could be expanded in future research to validate these results. In addition, inherent errors in marker-based kinematic data could affect the precision of the findings, particularly in patients with characteristic bony changes associated with pronovalgus and supovarus deformities.

5. Conclusion

The integration of MFPCA with k-means clustering resulted in the identification of six functional foot types. These clusters provide insights into foot alignment patterns in children with CP, thereby enhancing clinical understanding and informing treatment decisions. This stratification into clusters aids in developing personalized treatment plans, potentially improving mobility and quality of life. Our findings underscore the utility of MFPCA in clinical research, offering a comprehensive approach to assess foot deformities and guide interventions. This methodology not only facilitates diagnosis and treatment but also enriches the understanding of CP-related foot deformities, contributing to improved patient care and outcomes.

CRediT authorship contribution statement

Jeffrey S. Shilt: Writing – review & editing, Project administration, Methodology, Conceptualization. **Eric Dugan:** Writing – review & editing, Writing – original draft, Visualization, Validation, Software, Project administration, Methodology, Investigation, Formal analysis, Data curation, Conceptualization. **Amy E. Barbuto:** Writing – review & editing, Writing – original draft, Investigation, Conceptualization. **Cara M. Masterson:** Writing – review & editing, Software, Methodology, Formal analysis, Data curation.

Declaration of Competing Interest

None

Acknowledgements

Not Applicable

Appendix A. Supporting information

Supplementary data associated with this article can be found in the online version at doi:10.1016/j.gaitpost.2024.05.032.

References

[1] J.R. Davids, J. Shilt, R. Kay, T. Dreher, B.J. Shore, J. McCarthy, W. Shrader, K. Graham, M. Veerkamp, U. Narayanan, H. Chambers, T. Novacheck, J. Rhodes, A. Van Campenhout, K. Pierz, T. Theologis, E. Rutz, Assessment of foot alignment and function for ambulatory children with cerebral palsy: results of a modified Delphi technique consensus study, J. Child. 'S. Orthop. 16 (2022) 111–120, https://doi.org/10.1177/18632521221084183.

[2] J.R. Davids, The foot and ankle in cerebral palsy, Orthop. Clin. North Am. 41 (2010) 579–593, https://doi.org/10.1016/j.ocl.2010.06.002.

[3] K.M. Kruger, K.A. Konop, J.J. Krzak, A. Graf, H. Altiok, P.A. Smith, G.F. Harris, Segmental kinematic analysis of planovalgus feet during walking in children with cerebral palsy, Gait Posture 54 (2017) 277–283, https://doi.org/10.1016/j.gaitpost.2017.03.020.

[4] J. Amene, J.J. Krzak, K.M. Kruger, L. Killen, A. Graf, H. Altiok, P.A. Smith, G. F. Harris, Kinematic foot types in youth with pes planovalgus secondary to cerebral palsy, Gait Posture 68 (2019) 430–436, https://doi.org/10.1016/j.gaitpost.2018.12.026.

[5] J. Hamel, H. Hörterer, N. Harrasser, Is it possible to define reference values for radiographic parameters evaluating juvenile flatfoot deformity? A case-control study, BMC Musculoskelet. Disord. 21 (2020) 838, https://doi.org/10.1186/s12891-020-03854-6.

[6] H. Böhm, L. Döderlein, A. Fujak, C.U. Dussa, Is there a correlation between static radiographs and dynamic foot function in pediatric foot deformities, Foot Ankle Surg. 26 (2020) 801–809, https://doi.org/10.1016/j.fas.2019.10.006.

[7] A.K. Buldt, G.S. Murley, P. Levinger, H.B. Menz, C.J. Nester, K.B. Landorf, Are clinical measures of foot posture and mobility associated with foot kinematics when walking, J. Foot Ankle Res. 8 (2015) 63, https://doi.org/10.1186/s13047-015-0122-5.

[8] J.H. Lee, I.Y. Sung, J.Y. Yoo, Clinical or radiologic measurements and 3-D gait analysis in children with pes planus, Pediatr. Int. 51 (2009) 201–205.

[9] H. Böhm, C. Oestreich, R. Rethwilm, P. Federolf, L. Döderlein, A. Fujak, C.U. Dussa, Cluster analysis to identify foot motion patterns in children with flexible flatfeet using gait analysis—A statistical approach to detect decompensated pathology, Gait Posture 71 (2019) 151–156, https://doi.org/10.1016/j.gaitpost.2019.04.028.

[10] J.J. Krzak, D.M. Corcos, D.L. Damiano, A. Graf, D. Hedeker, P.A. Smith, G.F. Harris, Kinematic foot types in youth with equinovarus secondary to hemiplegia, Gait Posture 41 (2015) 402–408, https://doi.org/10.1016/j.gaitpost.2014.10.027.

[11] N. Portinaro, A. Leardini, A. Panou, V. Monzani, P. Caravaggi, Modifying the Rizzoli foot model to improve the diagnosis of pes-planus: application to kinematics of feet in teenagers, J. Foot Ankle Res. 7 (2014) 57, https://doi.org/10.1186/s13047-014-0057-2.

[12] H. Böhm, C.U. Dussa, Clinical, radiographic and gait parameters associated with medial arch pain in the flexible pediatric flatfoot, S1067251623000133, J. Foot Ankle Surg. (2023), https://doi.org/10.1053/j.jfas.2023.01.008.

[13] C.M. Kerr, J. Stebbins, T. Theologis, A.B. Zavatsky, Static postural differences between neutral and flat feet in children with and without symptoms, Clin. Biomech. 30 (2015) 314–317, https://doi.org/10.1016/j.clinbiomech.2015.02.007.

[14] N.J. Nahm, S.S. Sohrweide, R.A. Wervey, M.H. Schwartz, T.F. Novacheck, Surgical treatment of pes planovalgus in ambulatory children with cerebral palsy: static and dynamic changes as characterized by multi-segment foot modeling, physical examination and radiographs, Gait Posture 76 (2020) 168–174, https://doi.org/10.1016/j.gaitpost.2019.12.004.

[15] C. Bourdet, R. Seringe, C. Adamsbaum, C. Glorion, P. Wicart, Flatfoot in children and adolescents. Analysis of imaging findings and therapeutic implications, Orthop. Traumatol. Surg. Res. 99 (2013) 80–87, https://doi.org/10.1016/j.otsr.2012.10.008.

[16] T. Bloom, S. Sabharwal, Surgical management of foot and ankle deformities in cerebral palsy, Clin. Podiatr. Med. Surg. 39 (2022) 37–55, https://doi.org/10.1016/j.cpm.2021.09.001.

[17] K. Yoshida, D. Commandeur, S. Hundza, M. Klimstra, Detecting differences in gait initiation between older adult fallers and non-fallers through multivariate functional principal component analysis, J. Biomech. 144 (2022) 111342, https://doi.org/10.1016/j.jbiomech.2022.111342.

[18] K.E. Roach, V. Pedoia, J.J. Lee, T. Popovic, T.M. Link, S. Majumdar, R.B. Souza, Multivariate functional principal component analysis identifies waveform features of gait biomechanics related to early-to-moderate hip osteoarthritis, J. Orthop. Res. 39 (2021) 1722–1731, https://doi.org/10.1002/jor.24901.

[19] C. Happ, S. Greven, Multivariate functional principal component analysis for data observed on different (Dimensional) domains, J. Am. Stat. Assoc. 113 (2018) 649–659, https://doi.org/10.1080/01621459.2016.1273115.

[20] R Core Team, R: A Language and Environment for Statistical Computing, (2022). URL 〈https://www.R-project.org/〉.

[21] C. Happ-Kurz, Object-oriented software for functional data, J. Stat. Softw. 93 (2020), https://doi.org/10.18637/jss.v093.i05.

[22] J.O. Ramsay, Graves, Spencer, Hooker, Giles, fda: Functional Data Analysis, (2022). 〈https://CRAN.R-project.org/package=fda〉.

[23] C. Happ-Kurz, Multivariate Functional Principal Component Analysis for Data Observed on Different Dimensional Domains, J. Am.Stat. Assoc. (2022).

[24] A. Rozumalski, M.H. Schwartz, Crouch gait patterns defined using k-means cluster analysis are related to underlying clinical pathology, Gait Posture 30 (2009) 155–160, https://doi.org/10.1016/j.gaitpost.2009.05.010.

[25] J.R. Davids, T.W. Gibson, L.I. Pugh, Quantitative segmental analysis of weight-bearing radiographs of the foot and ankle for children: normal alignment, J. Pediatr. Orthop. 25 (2005) 769–776, https://doi.org/10.1097/01.bpo.0000173244.74065.e4.

[26] J.R. Davids, S.A. Tabaie, Foot and ankle motion in cerebral palsy, in: B. Müller, S. I. Wolf, G.-P. Brueggemann, Z. Deng, A. McIntosh, F. Miller, W.S. Selbie (Eds.), Handbook of Human Motion, Springer International Publishing, Cham, 2016, pp. 1–29, https://doi.org/10.1007/978-3-319-30808-1_58-1.